International Journal of Pharmaceutics 404 (2011) 281–288

Contents lists available at ScienceDirect

International Journal of Pharmaceutics

journal homepage: www.elsevier.com/locate/ijpharm

Pharmaceutical Nanotechnology

Retinyl acetate-loaded nanoparticles: Dermal penetration and release of the retinyl acetate

Sunatda Arayachukeat[a,b], Supason P. Wanichwecharungruang[c,*], Thapakorn Tree-Udom[a]

[a] Program of Petrochemistry and Polymer Science, Chulalongkorn University, Bangkok 10330, Thailand
[b] National Center of Petroleum, Petrochemicals and Advanced Materials, Chulalongkorn University, Bangkok 10330, Thailand
[c] Department of Chemistry, Faculty of Science, Chulalongkorn University, Payatai Road, Patumwan, Bangkok 10330, Thailand

ARTICLE INFO

Article history:
Received 2 September 2010
Received in revised form 26 October 2010
Accepted 11 November 2010
Available online 18 November 2010

Keywords:
Retinyl acetate
Encapsulation
Hair follicle
Polymeric carrier
Dermal penetration
Drug release

ABSTRACT

Retinyl acetate (RA) loaded polymeric nanoparticle (NP) carriers were prepared using two different single polymers, ethyl cellulose (EC) and poly (ethylene glycol)-4-methoxycinnamoylphthaloylchitosan (PCPLC). The stability of RA to aqueous solution and UVA light was significantly improved when encapsulated with PCPLC, whilst EC encapsulation gave some improved stability in water but showed no improved photostability. *Ex vivo* application of free RA and the RA-loaded PCPLC NPs onto the surface of the freshly excised skin from a baby mouse indicated a significantly slower skin absorption rate for the encapsulated RA. However, 100% retention of the encapsulated RA in the skin tissue was observed after 24 h. Confocal fluorescent analysis of the skin pieces applied with the RA-loaded PCPLC NPs indicated likely entry and accumulation of the PCPLC NPs and RA at the hair follicles. Release of RA from the PCPLC NP carriers was confirmed through the detection of an increasingly higher RA/PCPLC fluorescent signal ratio deeper into the dermis and away from the hair follicles.

1. Introduction

Vitamin A and many of its derivatives have been recognized as high-potential substances for the prevention and treatment of photoaging, severe acne and skin inflammation (Kligman et al., 1986; Leyden et al., 1989; Kligman, 1997; Cunliffe et al., 1997; Yamaguchi et al., 2005). Their biological activities include increasing the autolysis of keratinocytes, glycogen deposition and synthesis of collagen and elastin (Elias, 1986; Schwartz et al., 1991; Griffiths et al., 1993; Randolph and Simon, 1993). However, their application in dermatology is strongly limited by their induction of skin irritations and extreme instability (Isoe et al., 1972; Paquette and Kanaan, 1985; Manan et al., 1991; Crank and Pardijanto, 1995; Ioele et al., 2005; Xia et al., 2006). Since retinoic acid is classified as a drug in many countries and cannot be used in non-prescriptive cosmetic products, and also because of the instability of retinoic acid itself, many retinoic acid derivatives have been developed. Examples include retinol, retinaldehyde, retinyl palmitate (RP) and all *trans* retinyl acetate (RA). Amongst these many derivatives, RA is one of the popularly used derivatives in cosmetic products. However, the ability to induce skin irritation and the possible photo-induced DNA damage and photocytotoxicity of the ester form of retinoic acid, as well as its instability are known to exist (Yan et al., 2005). These factors then make the effective application without the use of high doses an essential requirement. Association of vitamin A derivatives with various delivery systems, such as liposomes (Sinico et al., 2005; Diaz et al., 2006), niosomes (Manconi et al., 2006), solid lipid nanoparticles (NPs) (Liu et al., 2007; Lim and Kim, 2002; Jee et al., 2006) and polymeric NPs (Kim et al., 2006; Ourique et al., 2008), has been proposed as methods to help improve their stability, solubility and efficiency. However, most reported systems showed only a very limited loading ability (0.1–0.5%, 0.10–4.89% and 4.76–17.35% (w/w) for liposomes, solid lipid NPs and polymeric NPs, respectively) and a limited improvement in the vitamin A (derivative) stability. Therefore, a carrier system with better RA loading characteristics and an improved ability to protect the encapsulated RA from photodegradation is still needed.

One of the many physiological functions of skin is protection, for example, against water loss, invasion of microorganisms and contamination from environmental substances. Therefore, percutaneous absorption of a drug without allowing other environmental agents in and without damaging the skin is a challenge. Nevertheless, we believe that a new drug delivery system that can target drug molecules to specific skin layers or even to the systemic circulation, by simple topical application, can be developed. At present it is known that (i) the stratum corneum is the least permeable layer of mammalian skin (Scheuplein and Blank, 1971), (ii) the intercellular pathway greatly predominates over the intracellular pathway for the penetration of most topically applied substances except water,

* Corresponding author. Tel.: +66 2 2187634; fax: +66 2 2541309.
E-mail address: psupason@chula.ac.th (S.P. Wanichwecharungruang).

0378-5173/$ – see front matter © 2010 Elsevier B.V. All rights reserved.
doi:10.1016/j.ijpharm.2010.11.019

(iii) hair follicles are another important penetration route (Patzelt et al., 2008). Domination amongst the three routes depends not only on the drug's physico-chemical properties, such as its solubility, diffuse-ability and molecular size, but also on the formulation and delivery system used.

Upon skin application, the stability of polymeric carriers differs considerably from conventional small surfactant molecule micelles (conventional emulsion systems) and vesicles (liposomes and niosomes). Polymeric NP carriers usually are not collapsible when dry and so the active molecules typically stay in the polymeric NPs on the surface of the skin after topical application and so should still be protected from environmental threats (e.g. water and oxygen). In contrast, with the small surfactant molecule carriers, the particles easily collapse upon drying and so the active molecules are directly in contact with the skin and also are exposed to various environmental threats. As a result, the skin penetration of drugs loaded in polymeric NPs differs from those in the conventional surfactant systems. Recently, the accumulation of polymeric NPs with a diameter of 20–320 nm was reported (Alvarez-Román et al., 2004; Lademann et al., 2007). Lademann et al. (2007) reported that the NP-encapsulated dye stayed at the hair follicles of the porcine skin for up to 10 days whilst the free dye could only be detected for up to 4 days. These findings suggest that hair follicles could be used as a reservoir for the skin administration of active molecules. However, the release of drug molecules from the NP carriers situated at the hair follicles is an essential requirement of this approach and so whether it occurs and to what extent must be clarified.

Although the *in vitro* release of drugs encapsulated in polymeric NPs has been reported for many different carrier systems, the actual release of the drug from the carriers trapped in the skin tissue has never really been established in their unmodified state (Wosicka and Cal, 2010; Alvarez-Román et al., 2004). Rather, the limited existing reports usually involve either fluorescent-labeled carriers or fluorescent dyes used as model drugs or both (Stracke et al., 2006). To start to address this, here we investigated the *ex vivo* skin absorption of RA-encapsulated in polymeric NPs, together with the release of RA from the NPs situated inside the skin. The work reported here also includes the ability to fabricate RA loaded polymeric NP carriers with a high RA loading, and an improved aqueous RA stability and RA photostabilty using UV absorptive chitosan. In addition, the use of confocal fluorescent laser spectroscopy to separately follow the drug and the polymeric carriers in the *ex vivo* skin tissue is demonstrated.

2. Materials and methods

2.1. Materials

RA and ethyl cellulose with ethoxy content of 48% and MW of 170,000 (EC, Fig. 1) were purchased from Sigma–Aldrich (St. Louis, MO, USA). Poly (ethylene glycol)-4-methoxycinnamoylphthaloylchitosan (PCPLC, Fig. 1) was prepared as previously described from chitosan (Anumansirikul et al., 2008).

2.2. RA encapsulation

RA-loaded PCPLC NPs were prepared by solvent displacement using dialysis under lightproof conditions. Thirty-milligrams of PCPLC were dissolved in 10.0 ml of DMSO to which 30, 20 or 10 mg of RA was added so as to yield polymer: RA (w/w) ratios of 1:1, 1.5:1 and 3:1. Each solution was dialyzed against water (five changes of 1 L each) using a regenerated cellulose membrane (MWCO of 12,400) with a 75 mm flat width, 17.9 ml cm^{-1} volume capacity (Membrane Filtration Products, Seguin, TX, USA). The suspension in the dialysis bag was then collected and its final volume was adjusted to 30 ml with water. The obtained RA-loaded NPs were then subjected to scanning electron microscopy (SEM, JEM-6400, JEOL, Japan), transmission electron microscopy (TEM, JEM-2100, JEOL, Japan), dynamic light scattering (DLS, Mastersizer S, Nano series model, Malvern Instruments, Worcestershire, UK) and surface charge (ζ, Zetasizer, Malvern Instruments) based analyses. Dry particles were obtained by freeze-drying (Freeze-Dry/Shell Freeze System Model 7753501, Labconco Corp., Kansus, MI, USA) the aqueous suspension. RA-loaded EC NPs were prepared similarly, except with EC and acetone used in place of the PCPLC and DMSO, respectively.

2.3. Encapsulation efficiency (EE) and RA loading

To extract the loaded RA out from the EC or PCPLC NP carriers, 1 ml of the freshly prepared RA-loaded NP suspension was centrifugally filtered through a MWCO 100,000 membrane (Amicon Ultra-15, Millipore, Billerica, MA, USA) and the obtained solid was soaked in 5 ml ethanol for 30 min at 25 °C under lightproof conditions, followed by 10 min sonication (40 kHz) at the same temperature. The suspension was then centrifugally filtered through a MWCO 100,000 membrane and the ethanol extract (liquid filtrate) was collected and subjected to quantitative analysis by UV-absorption spectrophotometry (UV 2500 UV-vis spectrophotometer, Shimadzu Corporation, Kyoto, Japan) with the aid of a calibration curve constructed from freshly prepared RA standard solutions. The encapsulation efficiency (%EE) and loading capacity (%loading) were then calculated using Eqs. (1) and (2), respectively.

$$\%\mathrm{EE} = \frac{\text{weight of encapsulated RA}}{\text{weight of RA initially used}} \times 100 \quad (1)$$

$$\%\text{RA loading} = \frac{\text{weight of encapsulated RA}}{\text{weight of the RA-loaded particles}} \times 100 \quad (2)$$

2.4. Stability of the encapsulated RA under lightproof condition

The stability of each encapsulated RA sample, and the free RA solution, was evaluated under a normal aqueous environment by monitoring the RA concentration of the freshly prepared RA-loaded NP suspension over three months under lightproof conditions. Twenty-five milliliters of each freshly prepared suspension of RA-loaded EC or PCPLC NPs (RA concentration of 300 ppm), as well as a 300-ppm free RA solution for comparison, were kept in a lightproof glass container at 30 °C. At appropriate times, a 1.0 ml aliquot was withdrawn and centrifugally filtered. The obtained solid was soaked in ethanol, sonicated, filtered and the ethanol extract was quantitatively analysed for RA content by UV-absorption spectrophotometry, all as detailed above. The experiments were done in triplicate and the data were subjected to Kolmogorov–Smirnov analysis.

2.5. Photostability of the encapsulated RA

The freshly prepared suspension of RA-loaded EC3 or PCPLC3 NPs (RA final concentration of 300 ppm) was exposed to broadband UVA radiation (320–400 nm, generated by an F24T12/BL/HO PUVA lamp, irradiances measured using UVA-400 C power meter, National Biological Corporation, Twinsburg, OH, USA) at 0, 7.8, 15.4, 30.7 and 45.9 J cm^{-2}. At each exposure, the UV spectrum was recorded. A freshly prepared free RA solution (300 ppm in ethanol) was also subjected to the same UVA exposure treatment for comparison. To control for the effect of simple scattering of the UVA light by the particles, the effect of adding empty (as in not RA-loaded) PCPLC NPs (1120 ppm) to a free RA solution (300 ppm), both at the same concentration as in the RA-loaded PCPLC NP trials, on the photostability of free RA was evaluated in otherwise

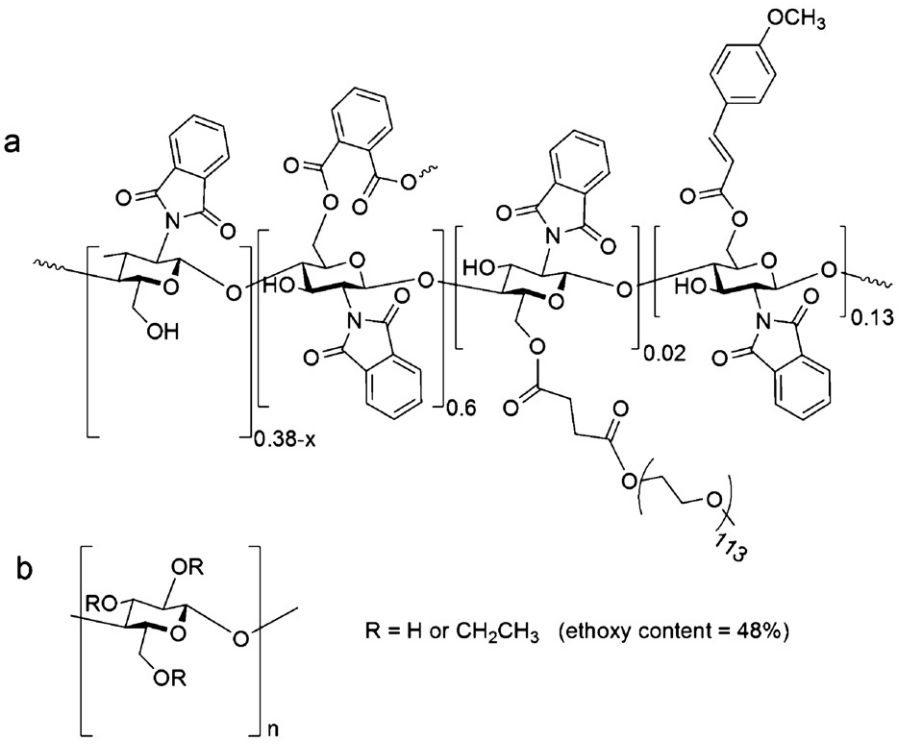

Fig. 1. Chemical structures of (a) PCPLC and (b) EC.

the same manner. The experiments were done in triplicate and a Kolmogorov–Smirnov test was used to indicate if the photostability of the samples was significantly different.

2.6. Ex vivo skin absorption of encapsulated RA

All animal experiments were performed under permission from the National Laboratory Animal Centre (Nakhon Pathom, Thailand).

The abdominal skin was freshly excised surgically from a nine-day-old-baby-mouse (*M. musculus* Linn.), purchased from the National Laboratory Animal Centre. The mouse skin, comprises epidermis and dermis and with a full thickness of approximately 450–600 μm, was cut into approximately 2.0 cm × 2.0 cm pieces.

The *ex vivo* skin penetration study of the encapsulated RA was conducted at 37 °C using a Franz diffusion cell with a 13.0 ml capacity receptor compartment and a 2.27 cm^2 diffusion area. The receptor medium was isotonic phosphate-buffered saline, pH 7.4 (PBS), supplemented with 1% (w/v) Tween 20, and it was constantly stirred during the experiment. The experiment was initiated by dropping 1.0 ml of the RA-loaded NP suspension (RA concentration = 999 ppm) into the upper compartment, directly onto the mounted skin (RA final coverage = 0.44 mg cm^{-2}). At 1, 2, 4, 6, 18 and 24 h later, 1.0 ml of the receptor fluid was withdrawn and replaced with fresh receptor medium. To eliminate variances due to differences in the permeability of skin from different mice, the penetration of each sample was compared to the penetration of the free RA solution derived from using skin from the same mouse, to standardize the results. To determine the amount of unabsorbed RA on the skin at 2 h and 24 h post application, 5.0 ml of the fresh receptor medium was dropped into the upper compartment of the diffusion cell, directly onto the mounted skin. The Franz cell was gently agitated and then the liquid was quickly withdrawn and subjected to RA quantification. The stability of the RA solution (in the receptor medium) was monitored for 24 h by periodically subjecting the solution to UV absorption analysis. The concentration of RA in each aliquot of the withdrawn receptor fluid was determined by UV/vis spectrophotometry at 325 nm, with the aid of a calibration curve. The experiment was performed with triplicate replications under light-proof conditions.

To distinguish between the RA absorbed into the skin from that which was degraded, the stability of RA in the receptor medium was also evaluated. The free RA solution and the RA-loaded PCPLC3 NP dispersion, both at a RA concentration of either 999 or 333 ppm, in the receptor medium, was kept under lightproof conditions and aliquots were periodically withdrawn and subjected to UV–visible absorption spectrophotometric analysis.

2.7. Ex vivo skin penetration and in-tissue-release of RA from PCPLC spheres

Confocal fluorescent microscopy (CFM) was used to capture the fluorescent signals of the PCPLC and the RA in the skin samples. The CFM system used was a Nikon Digital Eclipse C1-Si (Tokyo, Japan) equipped with Plan Apochromat VC 100×, BD Laser (408 nm, Melles Griot, Carlsbad, CA, USA), a Nikon TE2000-U microscope, a 32-channel-PMT-spectral-detector and Nikon-C1-Si software.

The experiment was started by placing 10 μl of the RA-loaded NP suspension (1000 ppm PCPLC and 333 ppm RA) onto the stratum corneum surface of a mouse skin piece (0.25 cm^2 area). The final coverage of PCPLC and RA on the skin was ~40 and ~13 μg cm^{-2}, respectively. The sample was then kept at 25 °C for 2 h before being subjected to CFM analysis. Fluorescent spectral signals at 420–750 nm were collected from the skin tissue at various depths starting from ~40 μm (from the stratum corneum surface) down to ~45 μm depth. The obtained spectra of each pixel were then unmixed into RA, PCPLC and skin auto-fluorescent components using chemometric analysis (image algorithms) based on the spectral database constructed from fluorescent spectra of standard PCPLC, standard RA and the skin tissue, through the Nikon-C1-Si software (Nikon, Tokyo, Japan). Images indicating locations of RA and PCPLC in the skin tissue were then constructed using the obtained resolved signals.

3. Results and discussion

3.1. RA encapsulation

The encapsulation of RA within EC and PCPLC NPs (Fig. 1) was successfully achieved by solvent displacement to obtain NPs of various RA loadings (Table 1). The SEM and TEM based images revealed spherical NPs (Fig. 2), and from these images the dry NP diameters were evaluated (Table 1). As the RA:polymer (w/w) ratio, and so the resultant %RA loading levels, increased then so the EE and the absolute value of the negative ζ decreased, whilst, as expected, the size of the NPs (both dry and hydrodynamic) increased. The result clearly indicated that the higher loading capacity afforded by increasing the RA to polymer (w/w) ratio during the encapsulation process was offset by the increased size of the NPs obtained and the decreased EE (%) and ζ of the NPs. To obtain RA-loaded PCPLC NPs with an acceptable ζ (<−20 mV), so as to result in minimal aggregation in water, would required the RA loading to not exceed ~21% (PCPLC3, Table 1). However, with EC as the polymeric shell material, NPs with as high a RA-loading of 45.7% (w/w) still showed acceptable ζ values (−26 to −32 mV). In this case, the effective and stably water dispersion of PCPLC3 and EC3 NPs agreed well with their highly negative ζ values observed in aqueous medium. Interestingly, but expectedly, as the polymer wall material was changed from EC to PCPLC, so the discrepancy between the dry (SEM) and hydrated NP size (obtained from DLS) estimates increased, suggesting a greater swelling in an aqueous environment for the PCPLC encapsulated NPs than that for the EC ones (Table 1). In fact, the swelling of chitosan and modified chitosan polymers in water is well known, whilst EC polymer is known to show very low amounts of swelling in water.

3.2. Stability of the encapsulated RA under lightproof conditions

Unencapsulated (free) RA showed an extreme instability in water under ambient conditions. However, after being encapsulated, the RA stability increased significantly (Fig. 3). As confirmed by Kolmogorov–Smirnov statistical analysis at the 99% significance level, within the PCPLC polymer types, the degradation kinetics of NPs with different RA loadings (PCPLC1–3) were significantly different, with the lowest RA loading level (PCPLC3) giving the slowest RA degradation rate. All three RA-loaded PCPLC NPs showed a significantly increased RA stability from the free RA. The increased stability of RA upon encapsulation under lightproof conditions was likely to be the result of RA being shielded from reactive oxygen species. With lower RA loadings, the protection of RA molecules should be greater as the polymer shield would be thicker.

In contrast, the same statistical analysis indicated that the three RA-loaded EC NPs (EC1–3) gave a similar RA stability, but they showed a significantly higher RA stability compared to that seen for the free RA. This implied that although the encapsulation into EC NPs could give some protection to RA, the protection was not load dependent. When comparing between the RA-loaded EC3 and PCPLC3 NPs, PCPLC3 obviously out performed EC3. Amongst the six RA-loaded NPs tested (EC1–3 and PCPLC1–3), only PCPLC3 NPs could retain approximately 40% of the loaded RA when kept as a water suspension for a period of 60–90 days, compared to 15–0% for the same time period for the other five samples. Of these five NP preparations, EC1–3 and PCPLC2 showed good RA protection during the first week as compared to the free RA, whilst PCPLC1 showed significant protection for only one day. The low protection of PCPLC1 could be attributed to its high RA-loading, since a lower RA-loading level would mean more polymer chains to shield the RA molecules from being attacked by the surrounding water and oxidizing agents, such as oxygen molecules, which can cause chemical degradation of the RA molecules [15]. It should be noted here that, the stability experiment was carried out with the test material being suspended in water medium, since this is typically the most appropriate medium for skincare applications. The result is encouraging that the PCPLC NP carrier could be used to encapsulate RA and the RA-loaded NPs with a RA loading of 21% could be dispersed in water with an approximately 40% RA stability improvement over a three month without the use of any antioxidant or surfactant.

The very basic "like dissolves like" rule could be used to explain the formation and aqueous stability of the prepared encapsulated RA. During the self-assembling of RA-loaded PCPLC NPs, hydrophobic RA molecules would try to position themselves to have minimal interaction with the polar water molecules, thus they should be directed towards the center of the PCPLC spheres. The PCPLC chains then organized themselves in such a way that the hydrophobic moieties have minimal contact with water, whilst their hydrophilic counterparts have a maximum interaction with the polar water medium. This arrangement not only pushed the RA molecules inside the spheres, but also made the spheres dispersible in water. Thus, a hydrophobic–hydrophilic gradient would be created with the hydrophobicity being more pronounced at the center of the spheres and the hydrophilicity more pronounced towards the surface of the spheres in an aqueous medium. The swelling of PCPLC should, therefore, be more pronounced towards the surface of the spheres. With higher RA loadings, there would not be enough hydrophobic moieties of the polymer to interact with them. Therefore, the RA molecules left in contact with the swelling PCPLC chain segments would increase, leading to the load-dependent stability observed above. The RA molecules with good contacts with the swelling PCPLC chains could then be easily and quickly attacked by the water soluble reactive oxygen species. As a result, a sharp drop in the amount of RA was observed during the first few days (Fig. 3b). In contrast, those RA molecules at the hydrophobic center were quite stable because the aqueous reactive oxygen species were not able to reach them.

The scenario was quite different for the EC NP carriers where a load-independent RA stability was observed (Fig. 3a). With the smaller hydrophobic moieties of the EC polymer compared to those of the PCPLC polymer (ethoxy moieties in EC versus N-phathaloyl and *p*-methoxycinnamoyl moieties in PCPLC, Fig. 1), the hydrophobic shielding of the loaded RA in the PCPLC NPs was more pronounced than that in the EC NPs. The load-independent stability of RA implied that the RA molecules in the EC1–3 NPs had similar protection (interaction) from the ethoxy groups of the EC chains. The steady degradation of RA over time supports the notion of a steady but slow access of reactive oxygen species to the encapsulated RA molecules, and this agreed well with the model of a similar interaction between RA and the ethoxy groups regardless of the RA position in the spheres.

3.3. Photostability of the encapsulated RA

Since it is known that RA degrades quickly with UVA radiation, we investigated if encapsulation could lessen such photodegradation. Because RA-loaded PCPLC3 NPs showed the highest improvement in RA stability under lightproof conditions, their photoprotection ability was investigated. For comparison, RA-loaded EC3 NPs, which has a similar RA-loading level to PCPLC3, were also tested. Since the experiment was carried out with the samples in the form of an aqueous suspension, it should be noted here that the duration of the photostability test of 90 min should allow observation of the degradation caused by the UVA radiation only, without the added effect of aqueous instability. This is because under the lightproof, but otherwise the same conditions, both EC3 and PCPLC3 NPs showed insignificant RA degradation over a 90 min period (Fig. 3).

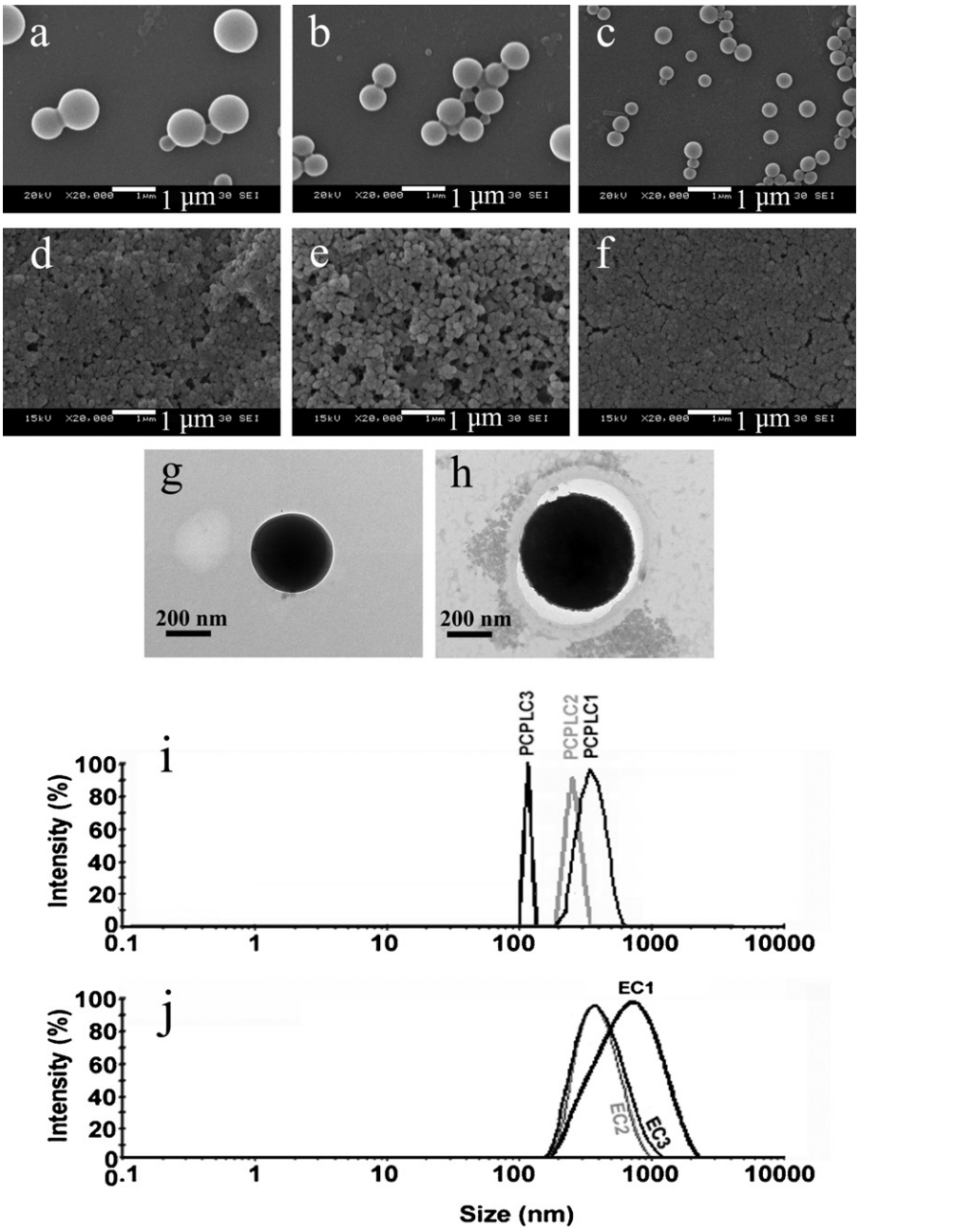

Fig. 2. Representative SEM photographs of RA-encapsulated NPs: (a) EC1, (b) EC2, (c) EC3, (d) PCPLC1, (e) PCPLC2 and (f) PCPLC3 N; representative TEM photographs of RA-encapsulated NPs: (g) EC3 and (h) PCPLC3; and hydrodynamic size distribution profiles of RA-encapsulated NPs: (i) PCPLC1–3 and (j) EC1–3. The composition of each NP type is given in Table 1.

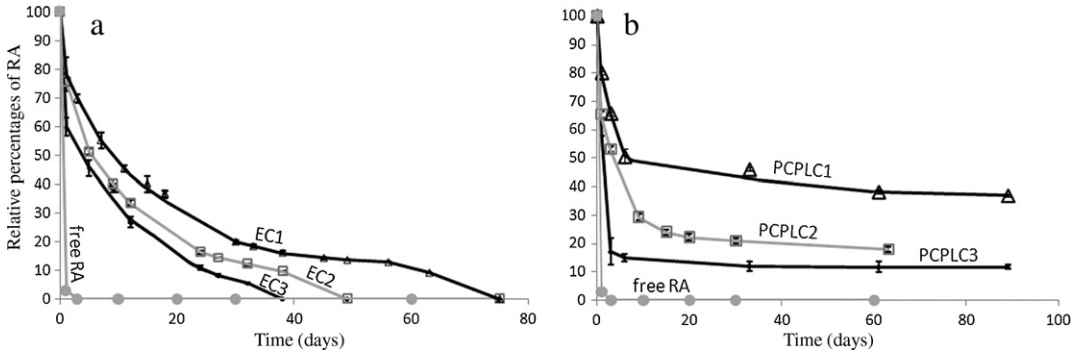

Fig. 3. Stability profiles of free RA and RA encapsulated in NPs of either (a) PCPLC or (b) EC, in an aqueous environment over time. Data are shown as the mean ± 1 S.D. and are derived from at least three repeats.

Table 1
Characteristics of RA encapsulated particles prepared at various polymer: RA (w/w) ratios.

Polymer	RA:polymer (w/w) ratio	Diameter (nm) (dry particles) mean ± S.D.	Hydrodynamic diameter (nm)	ζ (mV) mean ± S.D.	%EE mean ± S.D.	%RA loading mean ± S.D.
EC1	1:1	705.3 ± 141.9	673.9	−25.7 ± 0.1	84.7 ± 5.5	45.7 ± 1.8
EC2	1:1.5	602.7 ± 89.7	418.1	−27.6 ± 0.2	85.7 ± 10.5	36.3 ± 2.8
EC3	1:3	330.4 ± 50.6	406.1	−31.7 ± 0.3	90.1 ± 8.2	23.0 ± 1.6
PCPLC1	1:1	169.6 ± 43.7	519.9	−10.9 ± 0.9	61.0 ± 0.1	37.9 ± 0.1
PCPLC2	1:1.5	121.5 ± 13.9	446.7	−13.9 ± 1.3	65.3 ± 3.1	30.3 ± 0.9
PCPLC3	1:3	113.2 ± 27.1	226.9	−22.7 ± 2.3	77.9 ± 2.5	21.1 ± 0.2

Kolmogorov–Smirnov analysis at the 99% significance level indicated no difference in the RA degradation between the free RA and the RA encapsulated in EC3 NPs, whilst a significantly slower RA degradation rate was observed in the PCPLC3 sample ($Z = 2.000$, Sig. = 0.0005, Fig. 4). Comparing between the EC and the PCPLC NP carriers, it was obvious that the latter provided a significantly higher level of RA photostability, which can be explained through the UVA absorption property of the PCPLC polymer itself (Anumansirikul et al., 2008). In other words, the PCPLC polymeric matrix could significantly screen out the UVA light from reaching the encapsulated RA. To make sure that the improvement of RA photostability in the PCPLC3 was not the result of light scattering caused simply by the presence of the NPs, an aqueous solution of RA added with empty PCPLC NPs (free RA + PCPLC), to the same amount each as in the tested RA-loaded-PCPLC NPs, was also evaluated. Kolmogorov–Smirnov analysis indicated a similar degree of photostability amongst the free RA, the EC3 and the free RA + PCPLC samples at the 99% confidence level (Fig. 4). Therefore, the observed improvement in the photostability of RA upon encapsulation into the UV absorptive polymeric PCPLC NPs is likely to be authentic rather than an artifact of, for example, light scattering by the PCPLC NPs in suspension.

Although the photodegradation products of RA, together with the genotoxic and cytotoxic effects of RA, have not been reported, retinyl palmiate (RP, structure closely similar to RA) was reported to produce anhydroretinol and 5,6-epoxy-retinyl palmitate upon exposure to UVA radiation (Cherng et al., 2005). These two photodegradation products together with RP itself could induce DNA damage and were cytotoxic upon UVA exposure (Yan et al., 2005). Therefore, it is of great importance to ensure that the topically applied RA or RP is still well protected from light after being applied onto the skin. Therefore, the use of a UV-absorptive polymeric carrier should be beneficial.

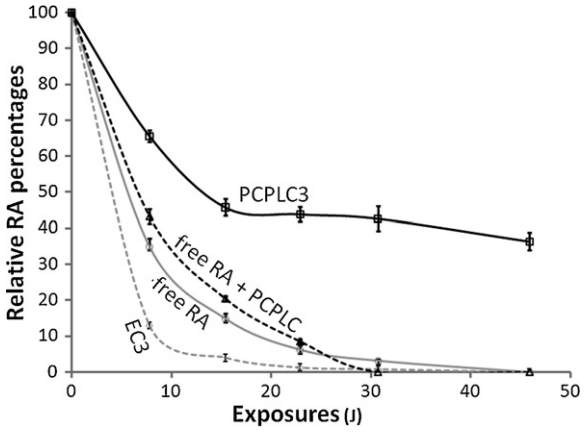

Fig. 4. Photostability profiles of free RA and RA encapsulated in NPs of either PCPLC at a 21.1% RA-loading (PCPLC3), or EC at 23.0% RA-loading (EC3), and free RA containing unloaded PCPLC NPs (free RA + PCPLC) in aqueous medium, when subject to the indicated UVA light exposure dose over 90 min. Data are shown as the mean ± 1 S.D. and are derived from at least three repeats.

3.4. Ex vivo skin absorption of encapsulated RA

Using a Franz diffusion cell set up, an *ex vivo* experiment was carried out to compare the transdermal penetration of the free RA, and the PCPLC encapsulated RA (PCPLC3), through the abdominal skin (composed of both dermis and epidermis) freshly excised from a nine-day-old baby mouse (*M. musculus* Linn.). First, the stability of the free RA and the encapsulated RA in the medium (isotonic PBS, with 1% (w/v) Tween 20) used in the experiment under lightproof conditions, was investigated. After 24 h, a 12 ± 1.3% degradation of the total amount of RA was observed for the free RA whilst no degradation at all was seen in the PCPLC3 encapsulated RA NPs. It is obvious that the free RA was significantly more stable in the PBS/Tween 20 release medium compared to that in pure water (compare above to Fig. 3), and this was likely to be the result of the non-ionic surfactant molecules (polysorbate or Tween 20) (Hwang et al., 2004). The encapsulation of the RA molecules into the polysorbate micelles could help shielding the RA from various water-soluble reactive species, thus making the compound more stable. The stability of the free RA in this medium allowed the Franz cell diffusion experiment to be conducted for a period of 24 h.

It should be mentioned here that, although surfactant micelles can help increase the stability of RA (Hwang et al., 2004), such micelles are not physically stable and will usually disintegrate upon drying (skin application), leaving the RA prone to photodegradation. The RA-loaded polymeric NPs (PCPLC3), however, are stable upon drying and, therefore, after skin application, RA should still be well protected from light.

The results of the Franz cell experiment under lightproof conditions clearly indicated that, at 0.44 mg cm^{-2} skin coverage, neither the free RA nor the RA in PCPLC3 NPs could significantly, if at all, penetrate fully across this full thickness skin, as no RA could be detected in the receptor fluid at 1, 2, 4, 6, 18 and 24 h post application. The surface of the skin was washed with fresh receptor medium at 2 and 24 h after the application, and the wash liquid was analysed for RA. For the free RA, no RA was found in the washes at 2 h after application. For the RA-loaded PCPLC3 NPs, 77.7 ± 5.1% of the applied amount of RA could be detected at 2 h after application but after 24 h no RA could be detected. With the pre-experiment of RA stability in the receptor medium discussed above, degradation of RA in the medium could be excluded and so it was concluded that by 24 h after application, all of the encapsulated RA was absorbed into the skin tissue. This assumes there is no significant degradation of RA on the skin by other means not present in the aqueous solution alone. If correct, this result indicated that the skin absorption of the encapsulated RA was slower than that of the free RA. The UV absorption profile of the wash fluid also indicated an insignificant amount of PCPLC polymer, thus it was possible that some of the encapsulated RA molecules absorbed into the skin were still encapsulated in the NP carriers. The absorbed but still encapsulated RA in the skin might not be available for the cells' uses, and so whether release from the NP carriers in the skin tissue occurred and to what extent requires clarification.

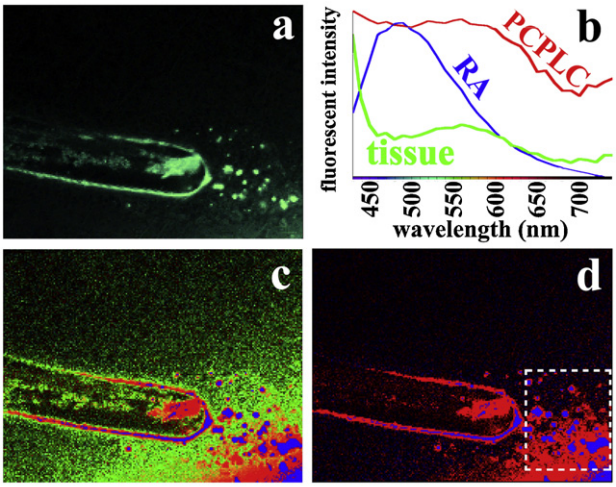

depth (μm)	fluorescent intensity (I)		I_{RA}/I_{PCPLC}
	I_{PCPLC}	I_{RA}	
40.0	2053.63	617.03	0.30
41.5	683.83	336.37	0.49
43.0	289.65	164.49	0.57
45.0	154.16	93.52	0.61

Fig. 5. Confocal fluorescent microscopy images showing skin penetration of RA-loaded PCPLC3 NPs and the release of RA into the tissue: (a) unresolved fluorescent image of the skin tissue at ~40 μm depth from the stratum corneum surface, 2 h after the RA-loaded PCPLC3 NP suspension was applied; (b) fluorescent spectrum of unencapsulated PCPLC NPs (red), RA (blue) and skin tissue (green); (c) superimposed image of the three resolved fluorescent images; (d) similar to (c) but only the PCPLC NPs (red) and RA (blue) signals are displayed. Fluorescent intensity of RA (I_{RA}) and that of PCPLC (I_{PCPLC}) at the area indicated in the dashed line-box in (d), at various depths from the stratum corneum, are shown in the table.

3.5. *Ex vivo skin penetration and in-tissue-release of RA from RA-loaded PCPLC NPs*

To further investigate the location of the penetrating PCPLC3 NPs and the release of the loaded RA in the skin tissue, RA-loaded PCPLC NPs (PCPLC3) were applied onto the stratum corneum surface of a nine day old baby mouse skin tissue at an average coverage of ~53 μg cm^{-2}, and then left at 25 °C for 2 h. The skin sample was then subjected to CFM analysis in which the fluorescent spectral signals from 420 to 750 nm at various skin depths were recorded (Fig. 5a). Since the fluorescent spectrum of RA is significantly different from that of the PCPLC polymer (Fig. 5b), it is possible to discriminate between them using chemometric analysis (image algorithm), and so be able to differentiate the location of the RA from the location of the PCPLC polymer. In addition, the auto-fluorescent spectrum of the tissue was significantly different from those of the two materials, allowing this signal component to be easily and clearly subtracted out in a similar manner. Therefore, the recorded fluorescent spectral signals of each pixel could be unmixed into RA, PCPLC and skin tissue signal components (Fig. 5c and d). The image of the resolved signals clearly indicated the presence of PCPLC and RA in the tissue. The highest intensity of fluorescent signals from both PCPLC and RA were found at the hair follicles, at ~40 μm depth from the stratum corneum surface. Accumulation of both the PCPLC polymer and RA at the hair follicle was very obvious. In addition, fluorescent signals from PCPLC and RA were also found at a high relative intensity at the internal root sheath along the hair shaft, suggesting that the hair follicle was the penetration route of the RA-loaded PCPLC NPs.

To investigate the release of RA from PCPLC NPs, the intensity of RA (I_{RA}) and PCPLC (I_{PCPLC}) fluorescent signals in the tissue area near the hair follicle (dashed line-box in Fig. 5d) at various depths, starting from 40 to 45 μm depth from the stratum corneum surface, were recorded (Table in Fig. 5). With increasing depth, the fluorescent signals from the two materials became weaker, corresponding well with the expectations of their slow diffusion into and through the dermis tissue. However, when the I_{RA}/I_{PCPLC} ratios were analysed, it was obvious that with increasing depth from the surface, the ratio increased significantly, e.g., the ratio at 45 μm depth was more than double that at 40 μm. This directly indicated a higher concentration ratio between RA and PCPLC with increasing depth, and implies the release of RA from the PCPLC NPs and the diffusion of the released RA molecules at a faster rate than the big and bulky PCPLC polymeric NPs (with or without RA loading).

It should be noted here that the free RA was more prone to photodegradation than that of the RA encapsulated in PCPLC NPs (as well as PCPLC itself), and this resulted in more photobleaching of free RA than RA-PCPLC or PCPLC NPs from the laser during the CFM acquisition. Nevertheless, under these experimental conditions, clear fluorescent signals from both the encapsulated and the released RA could still be obtained. Therefore, the increased RA:PCPLC signals at deeper dermis locations, in which the acquisition was carried out at later times than the upper dermis locations, truly indicates the release of the RA from the PCPLC spheres and a faster diffusion of the released RA molecules over the PCPLC.

The point should be made here that the observation was carried out at 2 h after the initial application time in order to minimize the interference from the RA released from the PCPLC3 NPs situated on the skin surface. Although it was concluded that the PCPLC3 NPs with RA inside could penetrate through the hair follicles, this did not mean that the release of the RA from the NPs situated on the skin could not happen. Moreover, the lower coverage of the PCPLC3 NPs used here (~53 μg cm^{-2}) compared to that in the Franz cell experiment (0.44 mg cm^{-2}) described above, was to ascertain that there would not be a lot of PCPLC3 left on the stratum corneum that would steadily release out RA into skin to interfere with the RA released from the skin absorbed PCPLC3 spheres. Although these scenarios are unlikely, since it was reported previously that an accumulation of retinyl ester in the dermis through topical application of unencapsulated material was negligible (Yan et al., 2006), this precaution was still taken. These careful conditions increase the confidence of the conclusion that RA-loaded PCPLC NPs could penetrate into the dermis, most likely *via* the hair follicles, and that the accumulated spheres at the hair follicles can release the encapsulated RA into the surrounding tissue. The released RA can then diffuse through the skin tissue at a faster rate than their polymeric carriers. This result agrees well with some recent reports that have stated that hair follicles represent a highly relevant and efficient penetration pathway and reservoir for topically applied substances (Wosicka and Cal, 2010; Lademann et al., 2008; Teichmann et al., 2007).

Taking into account the results from the Franz cell experiment and the CFM experiment, it can be concluded that (i) RA loaded PCPLC spheres can penetrate into the dermis layer *via* hair follicles, (ii) RA can be released from the PCPLC NPs trapped at the hair follicles, (iii) the RA release was slow as no RA could cross the full skin by 24 h after their application (see above comment). Nevertheless, the results here indicate that, with the use of proper polymeric NP carriers, drug delivery to the dermis layer can be achieved. Given that the dermis layer is usually vascularized then the confirmation of the release of the encapsulated compound from the carriers accumulated at the hair follicles thus suggests a

possible systemic administration of the drug (in this case RA) *via* topical application.

4. Conclusion

We have shown that the improved RA stability through nanoencapsulation was subject to the type of carrier used. The UV absorptive PCPLC NPs could improve both the aqueous stability and the photostability of RA and this improvement was load-dependent, whilst the EC NPs could improve only the aqueous stability. The Franz cell experiment indicated that the RA-loaded PCPLC NPs could be absorbed into the freshly excised skin of baby mice, albeit at a slower rate than the free RA. Since the PCPLC polymer and RA molecules possess a different fluorescent spectrum, chemometric analysis could be employed to resolve the two spectral signals from one another. As a result, the release of RA from the PCPLC NP carriers could be confirmed through the detection of an increasingly higher RA/PCPLC fluorescent signal ratio deeper into the dermis away from the hair follicles.

Acknowledgements

The authors thank the Thailand Research Fund, the Ratchadaphisesomphot endowment fund from Chulalongkorn University, the Thai Government Stimulus Package 2 (TKK2555) under the Project for Establishment of Comprehensive Center for Innovative Food, Health Products and Agriculture, for the financial support. The authors are also grateful for the English corrections from Robert Butcher of the Publication Counseling Unit, Faculty of Science, Chulalongkorn University.

References

Alvarez-Román, Naik, A., Kalia, Y.N., Guy, R.H., Fessi, H., 2004. Skin penetration and distribution of polymeric nanoparticles. J. Control. Release 99, 53–62.

Anumansirikul, N., Wittayasuporn, M., Klinubol, P., Tachaprutinun, A., Wanichwecharungruang, S.P., 2008. UV-screening chitosan nanocontainers: increasing the photostability of encapsulated materials and controlled release. Nanotechnology 19, e205101.

Cherng, S.-H., Xia, Q., Blankenship, L.R., Freeman, J.P., Wamer, W.G., Howard, P.C., Fu, P.P., 2005. Photodecomposition of retinyl palmitate in ethanol by UVA light-formation of photodecomposition products, reactive oxygen species, and lipid peroxides. Chem. Res. Toxicol. 18, 129–138.

Crank, G., Pardijanto, M.S., 1995. Photo-oxidations and photosensitized oxidations of vitamin a and its palmitate ester. J. Photochem. Photobiol. A: Chem. 85, 93–100.

Cunliffe, W.J., Caputo, R., Dreno, B., Förström, L., Heenen, M., Orfanos, C.E., Privat, Y., Aguilar, A.R., Meynadier, J., Alirezai, M., Jablonska, S., Shalita, A., Weiss, J.S., Chalker, D.K., Ellis, C.N., Greenspan, A., Katz, H.I., Kantor, I., Millikan, L.E., Swinehart, J.M., Swinyer, L., Whitmore, C., Czernielewski, J., Verschoore, M., 1997. Clinical efficacy and safety comparison of adapalene gel and tretinoin gel in the treatment of acne vulgaris: Europe and U.S. multicenter trials. J. Am. Acad. Dermatol. 36, S126–S134.

Diaz, C., Vargas, E., Gatjens-Boniche, O., 2006. Cytotoxic effect induced by retinoic acid loaded into galactosyl-sphingosine containing liposomes on human hepatoma cell lines. Int. J. Pharm. 325, 108–115.

Elias, P.M., 1986. Epidermal effects of retinoids: supramolecular observations and clinical implications. J. Am. Acad. Dermatol. 15, 797–809.

Griffiths, C., Russman, A.N., Majmudar, G., Singer, R.S., Hamilton, T.A., Voorhees, J.J., 1993. Restoration of collagen formation in photodamaged human skin by tretinoin (retinoic acid). New Engl. J. Med. 329, 530–535.

Hwang, S.R., Lim, S.J., Park, J.S., Kim, C.K., 2004. Phospholipid-based microemulsion formulation of all-trans-retinoic acid for parenteral administration. Int. J. Pharm. 276, 175–183.

Ioele, G., Cione, E., Risoli, A., Genchi, G., Ragno, G., 2005. Accelerated photostability study of tretinoin and isotretinoin in liposome formulations. Int. J. Pharm. 293, 251–260.

Isoe, S., Hyeon, S.B., Katsumura, S., Sakan, T., 1972. Photo-oxygenation of carotenoids. Ii. The absolute configuration of loliolide and dihydroactinidiolide. Tetrahedron Lett. 13, 2517–2520.

Jee, J.-P., Lim, S.-J., Park, J.-S., Kim, C.-K., 2006. Stabilization of all-trans retinol by loading lipophilic antioxidants in solid lipid nanoparticles. Eur. J. Pharm. Biopharm. 63, 134–139.

Kim, D.G., Jeong, Y.I., Choi, C., Roh, S.H., Kang, S.K., Jang, M.K., Nah, J.W., 2006. Retinol-encapsulated low molecular water-soluble chitosan nanoparticles. Int. J. Pharm. 319, 130–138.

Kligman, A.M., 1997. The treatment of acne with topical retinoids: one man's opinions. J. Am. Acad. Dermatol. 36, S92–S95.

Kligman, A.M., Grove, G.L., Hirose, R., Leyden, J.J., 1986. Topical tretinoin for photoaged skin. J. Am. Acad. Dermatol. 15, 836–859.

Lademann, J., Richter, H., Teichmann, A., Otberg, N., Blume-Peytavi, U., Luengo, J., Weiß, B., Schaefer, U.F., Lehr, C.-M., Wepf, R., Sterry, W., 2007. Nanoparticles—an efficient carrier for drug delivery into the hair follicles. Eur. J. Parm. Biopharm. 66, 159–164.

Lademann, J., Knorr, F., Richter, H., Blume-Peytavi, U., Vogt, A., Antoniou, C., Sterry, W., Patzelt, A., 2008. Hair follicles—an efficient storage and penetration pathway for topically applied substances: summary of recent results obtained at the center of experimental and applied cutaneous physiology, Charité – Universitätsmedizin Berlin, Germany. Skin Pharmacol. Phys. 21, 150–155.

Leyden, J.J., Grove, G.L., Grove, M.J., Thorne, E.G., Lufrano, L., 1989. Treatment of photodamaged facial skin with topical tretinoin. J. Am. Acad. Dermatol. 21, 638–644.

Lim, S.J., Kim, C.K., 2002. Formulation parameters determining the physicochemical characteristics of solid lipid nanoparticles loaded with all-trans retinoic acid. Int. J. Pharm. 243, 135–146.

Liu, J., Hu, W., Chen, H.B., Ni, Q., Xu, H.B., Yang, X.L., 2007. Isotretinoin-loaded solid lipid nanoparticles with skin targeting for topical delivery. Int. J. Pharm. 328, 191–195.

Manan, F., Guevara, L.V., Ryley, J., 1991. The stability of all-trans retinol and reactivity towards transition metals. Food Chem. 40, 43–54.

Manconi, M., Sinico, C., Valenti, D., Lai, F., Fadda, A.M., 2006. Niosomes as carriers for tretinoin: Iii. A study into the in vitro cutaneous delivery of vesicle-incorporated tretinoin. Int. J. Pharm. 311, 11–19.

Ourique, A.F., Pohlmann, A.R., Guterres, S.S., Beck, R.C., 2008. Tretinoin-loaded nanocapsules: preparation, physicochemical characterization, and photostability study. Int. J. Pharm. 352, 1–4.

Paquette, G., Kanaan, M.A., 1985. Degradation of retinyl acetate in simple solvent systems. Food Chem. 18, 211–231.

Patzelt, A., Antoniou, C., Sterry, W., Lademann, J., 2008. Skin penetration from the inside to the outside: a review. Drug Discov. Today: Dis. Mech. 5, e229.

Randolph, R.K., Simon, M., 1993. Characterization of retinol metabolism in cultured human epidermal keratinocytes. J. Biol. Chem. 268, 9198–9205.

Scheuplein, R.J., Blank, I.H., 1971. Permeability of the skin. Physiol. Rev. 51, 702–747.

Schwartz, E., Cruickshank, F.A., Mezick, J.A., Kligman, L.H., 1991. Topical all-trans retinoic acid stimulates collagen synthesis in vivo. J. Invest. Dermatol. 96, 975–978.

Sinico, C., Manconi, M., Peppi, M., Lai, F., Valenti, D., Fadda, A.M., 2005. Liposomes as carriers for dermal delivery of tretinoin: in vitro evaluation of drug permeation and vesicle–skin interaction. J. Control. Release 103, 123–136.

Stracke, F., Weiss, B., Lehr, C.M., Koenig, K., Schaefer, U.F., Schneider, M., 2006. Multiphoton microscopy for the investigation of dermal penetration of nanoparticle-borne drugs. J. Invest. Dermatol. 126, 2224–2233.

Teichmann, A., Heuschkel, S., Jacobi, U., Presse, G., Neubert, R.H.H., Sterry, W., Lademann, J., 2007. Comparison of stratum corneum penetration and localization of a lipophilic model drug applied in an o/w microemulsion and an amphiphilic cream. Eur. J. Pharm. Biopharm. 67, 699–706.

Wosicka, H., Cal, K., 2010. Targeting to the hair follicles: current status and potential. J. Dermatol. Sci. 57, 83–89.

Xia, Q., Yin, J.J., Wamer, W.G., Cherng, S.H., Boudreau, M.D., Howard, P.C., Yu, H., Fu, P.P., 2006. Photoirradiation of retinyl palmitate in ethanol with ultraviolet light-formation of photodecomposition products, reactive oxygen species, and lipid peroxides. Int. J. Environ. Res. 3, 185–190.

Yamaguchi, Y., Nagasawa, T., Nakamura, N., Takenaga, M., Mizoguchi, M., Kawai, S.-I., Mizushima, Y., Igarashi, R., 2005. Successful treatment of photo-damaged skin of nano-scale ultra particles using a novel transdermal delivery. J. Control. Release 104, 29–40.

Yan, J., Xia, Q., Cherng, S.H., Wamer, W.G., Howard, P.C., Yu, H., Fu, P.P., 2005. Photo-induced DNA damage and photocytotoxicity of retinyl palmitate and its photodecomposition products. Toxicol. Ind. Health 21, 167–175.

Yan, J., Xia, Q., Webb, P., Warbritton, A.R., Wamer, W.G., Howard, P.C., Boudreau, M., Fu, P.P., 2006. Levels of retinyl palmitate and retinol in the stratum corneum, epidermis, and dermis of female SKH-1 mice topically treated with retinyl palmitate. Toxicol. Ind. Health 22, 181–191.